

# Effect of calcination on the microstructures of titania nanoparticles prepared in W/O microemulsions

EUI JUNG KIM<sup>\*,§</sup>, SUNWOOK KIM<sup>\*</sup>, SUNG-HONG HAHN<sup>‡</sup>

<sup>\*</sup>Department of Chemical Engineering and <sup>‡</sup>Department of Physics, University of Ulsan, Ulsan 680-749, Korea

E-mail: ejkim@uou.ulsan.ac.kr

Monodispersed titania nanoparticles were prepared from reacting  $\text{TiOCl}_2$  with  $\text{NH}_4\text{OH}$  in water/Triton X-100/*n*-hexanol/cyclohexane microemulsions. The effect of calcination on the microstructures of the particles was investigated. The particles synthesized were amorphous, transformed into the anatase phase at 300°C, and further into the rutile phase at 850°C. The crystallite size of the particles was 9.7 to 35.6 nm in the temperature range between 300 and 900°C. Secondary particles, agglomerates of finer primary particles, were about 20 nm in size at 200°C and increased markedly by a factor of 10 to 20 at 900°C due to a significant interagglomerate densification. With increasing calcination temperature from 300 to 900°C, the specific surface area of the particles decreased rapidly from 317.5 to 8.4 m<sup>2</sup>/g, whereas the average pore radius increased considerably from 2.9 to 31.8 nm as the result of shrinkage of the agglomerates, destruction of the minute intercrystallite pores, and interagglomerate densification. © 2002 Kluwer Academic Publishers

## 1. Introduction

Titania powders find industrial applications such as pigments, fillers, opacifiers, catalytic supports, and photocatalysts. In most cases the titania particles are fabricated by the hydrolysis of  $\text{TiCl}_4$  in acidic solutions [1]. They also can be obtained from the gas-phase oxidation of  $\text{TiCl}_4$  [2, 3] or the hydrolysis of titanium alkoxides in alcoholic solutions [4].

Nanosized materials with grain sizes below 100 nm are of scientific interest because of improved physical properties resulting from the grain size reduced to the nanometer scale. The use of nanoparticles leads to lowering the sintering temperature and improving the sintering rate. Various chemical methods have been proposed to prepare nanosized particles with a narrow and controllable size distribution [5–7]. Water-in-oil (W/O) microemulsions have been successfully employed to produce monodisperse, high purity nanoparticles [8, 9]. In W/O microemulsions, an aqueous phase is dispersed as microdroplets (typically 5–50 nm in size) in a continuous oil phase. The reaction takes place inside the aqueous cores that control the final size of the particles. Once the particles attain the final size, the surfactant molecules are attached to the surface of the particles, thus stabilizing and protecting them against further growth.

In this work, monodispersed titania nanoparticles were prepared from reacting  $\text{TiOCl}_2$  with  $\text{NH}_4\text{OH}$  in W/O microemulsions consisting of Triton X-100,

*n*-hexanol, cyclohexane, and aqueous solution. The titania particles synthesized were characterized using FTIR, XRD, SEM, TEM, and BET techniques. The effect of calcination temperature on the microstructural features of the particles was explored.

## 2. Experimental

### 2.1. Materials

Triton X-100 as a surfactant and *n*-hexanol as a co-surfactant were purchased from Aldrich Chemical Co., cyclohexane and ammonia solution from Oriental Chemical Industries, and  $\text{TiCl}_4$  from Kanto Chemical Co. All reagents were used as received without further purification. Water used in the experiments was double-distilled and deionized.

### 2.2. Preparation of titania powders

Microemulsions were prepared by solubilizing different electrolytes into Triton X-100/*n*-hexanol/cyclohexane solutions. We took the method consisting in mixing two microemulsions (microemulsion I and microemulsion II) carrying the appropriate reactants in order to obtain titania particles [10]. The aqueous phase in microemulsion I was 1 M  $\text{TiOCl}_2$  solution, while the aqueous phase in microemulsion II was 6.5 M  $\text{NH}_4\text{OH}$  solution as a precipitating agent. Each microemulsion contained 10% aqueous solution, 20%

<sup>§</sup> Author to whom all correspondence should be addressed.

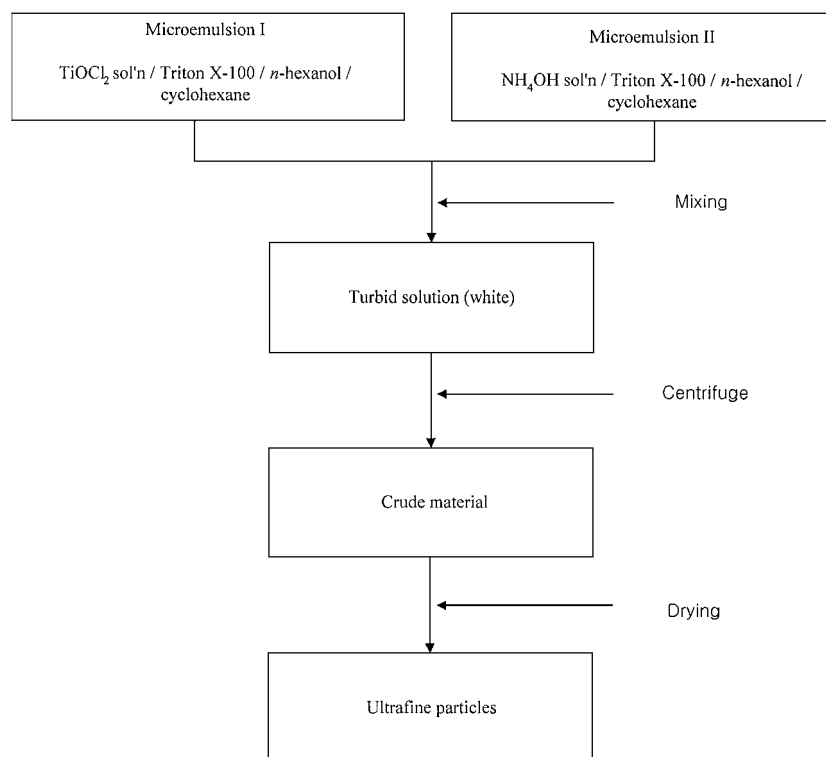


Figure 1 Flow chart of all steps involved in the synthesis of titania nanoparticles using W/O microemulsions.

Triton X-100, 15% *n*-hexanol, and 55% cyclohexane by mass. When  $\text{TiCl}_4$  is dissolved in water, the exothermic reaction explosively occurs leading to the formation of orthotitanic acid  $[\text{Ti}(\text{OH})_4]$  that disturbs homogeneous precipitation of the titania particles. We prepared a transparent  $\text{TiOCl}_2$  solution utilizing the method suggested by Kim *et al.* [11]. Microemulsions I and II were mixed in a jacketed Erlenmeyer flask with stirring in nitrogen. This led to the precipitation of the titania nanoparticles within the aqueous cores of the microemulsions. The particles formed in the constrained microemulsion microdroplets are fairly uniform and homogeneous. The reaction temperature was maintained at  $25^\circ\text{C}$  by circulating a coolant with a Lauda RC20B chiller.

The titania particles precipitated were separated in a Hanil HA-500 centrifuge at 10,000 rpm for 10 min and were then washed with ethanol and acetone consecutively to remove organics and surfactants from the particles. The particles were then dried at  $50^\circ\text{C}$  for about 20 hours. The flow chart showing the preparation of the titania particles is illustrated in Fig. 1. Dried particles were calcined in a Lindberg 55342-4 furnace at temperatures above  $200^\circ\text{C}$  to examine the transition of crystal phase and the crystallite size and morphology of the particles.

### 2.3. Powder characterization

Powder X-ray diffraction (XRD) was used for crystal phase identification and estimation of the crystallite size of each phase. XRD patterns were obtained with a Philips PW3710 diffractometer using  $\text{Cu } K_\alpha$  radiation at 30 kV and 20 mA. The particle size and morphology were analyzed by scanning electron microscopy (SEM). Transmission electron microscopy (TEM) was

used to study the primary particle size of the powders. TEM samples were prepared by ultrasonically dispersing the powders in ethanol prior to placing a drop of resultant suspension on a carbon-coated copper grid. TEM observations were performed using a Hitachi H-7100 transmission electron microscope. The specific surface area of the precipitates was measured with a Quantachrome Autosorb-1 nitrogen adsorption apparatus. The chemical structure of the particles was examined using an ATI Mattson Genesis Series Fourier transform infrared (FTIR) spectrophotometer.

### 3. Results and discussion

In the experiments of Chhabra *et al.* [10] who employed the same microemulsion system as ours, the concentrations of  $\text{TiOCl}_2$  and  $\text{NH}_4\text{OH}$  aqueous solutions were 0.3 and 1.2 M, respectively. However, we found that titania particles were precipitated in extremely small amounts at these concentration levels. In this work, the concentrations of  $\text{TiOCl}_2$  and  $\text{NH}_4\text{OH}$  aqueous solutions were typically 1.0 and 6.5 M, respectively. A clear microemulsion was not obtained if the concentration of  $\text{NH}_4\text{OH}$  aqueous solution was greater than 8.0 M since  $\text{NH}_4\text{OH}$  is acting as a lyotropic salt reducing the mutual solubility between water and surfactant [12].

Fig. 2 shows FTIR spectra for the titania particles calcined at various temperatures ranging from 300 to  $900^\circ\text{C}$ . The calcination was carried out at each temperature for 2 hours in air. It can be seen that at  $300^\circ\text{C}$  absorption peaks occurring in the range of  $900\text{--}1300\text{ cm}^{-1}$  almost disappeared denoting that most of organics were removed. Also, the intensities of absorption peaks at around  $3400$  and  $1620\text{ cm}^{-1}$ , respectively, reduced significantly. As the calcination temperature increased to  $500^\circ\text{C}$ , the intensities of these absorption

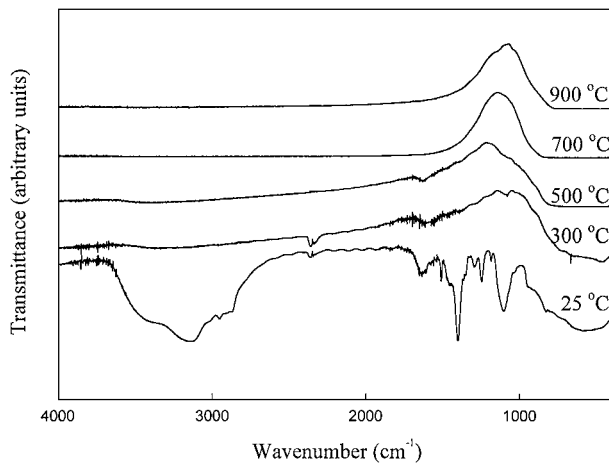


Figure 2 FTIR spectra for titania particles calcined at various temperatures.

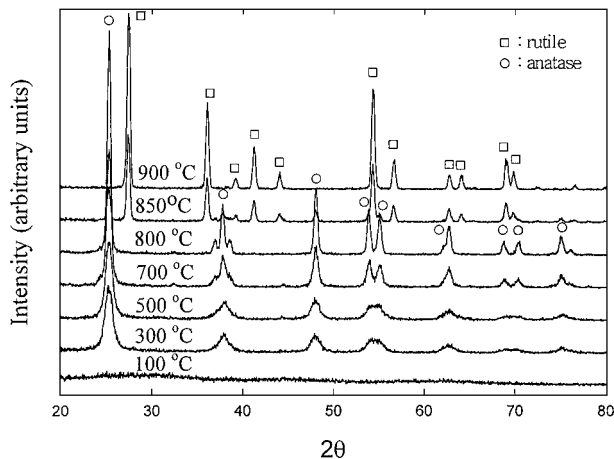


Figure 3 Effect of calcination on the crystal structure of titania particles.

peaks were further reduced. At temperatures above 700 °C, these peaks no longer appeared indicating that water and –OH bonds were completely removed from the particles.

The titania particles formed within the water pools of microemulsion were calcined for 2 hours in air at different temperatures between 100 and 900 °C to examine the phase transition by the powder XRD technique. Fig. 3 illustrates the XRD patterns of the particles calcined at different temperatures. The XRD data of the particles calcined at 100 °C indicate that they are amorphous.  $\text{NH}_4\text{Cl}$  is formed by the reaction between  $\text{NH}_4\text{OH}$  and  $\text{TiOCl}_2$  during the synthesis of the titania particles. The  $\text{NH}_4\text{Cl}$  peaks appeared in the XRD data of the particles calcined at 100 °C when washing of the precipitated particles with alcohol was insufficient. As seen in Fig. 3, the particles calcined at 300 °C were identified as nanocrystalline anatase. This result implies that the anatase phase began to form at 300 °C. Chhabra *et al.* [10] reported that the particles calcined at 400 °C were amorphous and the anatase phase began to form at 600 °C. In their experiments, the concentrations of  $\text{TiOCl}_2$  and  $\text{NH}_4\text{OH}$  aqueous solutions were 0.3 and 1.2 M, respectively, which are considerably low compared to those employed in our experiments (1.0 and 6.5 M). Accordingly, higher  $\text{TiOCl}_2$  and  $\text{NH}_4\text{OH}$  concentrations facilitate the precipitation of titania particles and the formation of anatase crystalline phase.

In Fig. 3, raising the calcination temperature from 300 to 800 °C resulted in an improvement in crystallinity without phase transition. On increasing the temperature to 850 °C, the intensities of the anatase peaks significantly reduced, but the rutile peaks appeared. This indicates that the transition from anatase to rutile took place. If the temperature increased further to 900 °C, the anatase peaks disappeared implying that the phase transition completed. Shannon and Pask [13] showed that the anatase-rutile transformation involves an overall contraction or shrinking of the oxygen structure and a co-operative movement of oxygen and titanium ions. This crystal phase transition has to overcome strain energy for the oxygen ions to reach their new configuration and the energy necessary to break the Ti-O bonds, thus it takes place at high temperatures. In the experiments of Chhabra *et al.* [10], the particles calcined at 900 °C were a mixture of both the anatase and rutile phases. Lal *et al.* [14] synthesized ultrafine titania particles in W/O microemulsions by hydrolysis of titanium diethylhexyl sulfosuccinate [Ti-DEHSS].

They found that the anatase-rutile transformation temperature was decreased from 650 to 500 °C as the concentration of Ti-DEHSS increased from 0.1 to 0.3 M. The above results suggest that higher reactant concentrations promote the transition of anatase to rutile lowering the phase transition temperature. It is known that if titania particles prepared are ultrafine and uniform in size, the rutile phase can be formed even at a temperature as low as 200 °C because of their high specific surface area and reactivity. Relatively higher  $\text{NH}_4\text{OH}$  concentration employed in this work may facilitate nucleation rates thus resulting in more nuclei. This, in turn, leads to smaller particles lowering the phase transition temperature. Furthermore, Ti-O-Ti bonds possibly break in highly alkaline solutions reducing the particle size [15].

The crystallite size of the particles can be determined from the broadening of corresponding XRD peaks by Scherrer's equation [16]

$$L = \frac{K\lambda}{\beta \cos \theta} \quad (1)$$

where  $L$  is the crystallite size,  $\lambda$  is the wavelength of X-ray radiation,  $K$  is usually taken as 0.94, and  $\beta$  is the angle width at half maximum height. The peaks of anatase (101) and rutile (110) occurred at  $2\theta = 25.3^\circ$  and  $27.4^\circ$ , respectively. The crystallite sizes of each phase present in the particles are listed in Table I. One

TABLE I XRD results for titania particles calcined at various temperatures for 2 hours

Calcination temp. (°C)	Crystallite size (nm)	
	Anatase	Rutile
300	9.7	–
500	9.8	–
700	18.7	–
800	28.5	–
850	30.3	34.5
900	–	35.6

can see that the crystallite size of the anatase phase was increased about 3 times as the calcination temperature increased from 300 to 850°C. Negligible grain growth occurred up to 500°C and the anatase grain size doubled at 700°C. This indicates that intra-agglomerate densification becomes significant at temperatures above 700°C. The size of the rutile crystallites calcined at 850°C was 34.5 nm and slightly increased to 35.6 nm at 900°C. Porter *et al.* [17] explored the effect of calcination on the microstructural characteristics of commercial Degussa P-25 titania. They found that the crystallite size of the anatase phase ranged from 20 to 40 nm at temperatures between 600 and 750°C. Therefore, the grain size of the particles synthesized in our experiments is relatively smaller than that of Degussa P-25 powders. They also observed that rapid grain growth began at 700°C, accelerated with further increase in temperature, and the grain size increased by a factor of 10 at 900°C compared to the original Degussa P-25 powders. Edelson and Glaeser [18] synthesized monosized titania particles by controlled hydrolysis of titanium ethoxide in ethanol. They found that titania particles synthesized were agglomerates of about 6-nm primary particles and that the anatase grain size approached 90 nm in 1 hour at 600°C. However, such a rapid increase in grain size was not observed in our experiments.

Fig. 4 shows TEM micrographs of the titania nanoparticles before and after calcination. In Fig. 4a, the TEM sample was prepared by diluting colloidal reaction solution with ethanol at a volume ratio of 1 to 10 and in Fig. 4b by ultrasonically dispersing 50 mg of the calcined particles in ethanol. TEM images show agglomerates of the primary nanoparticles. Some *ex situ* aggregation of the sample particles on the TEM

grid cannot, of course, be excluded. As seen in Fig. 4a, the primary particles of the as-prepared titania were so small that it was difficult to determine their accurate size from the TEM micrograph. The primary particles are, however, estimated to be within a few nm in size. The size of the as-prepared particles was also measured via dynamic light scattering and was typically about 3–5 nm, which is reasonably consistent with that observed in the TEM micrograph. The particle size distribution turned out to be very narrow. As shown in Fig. 4b, the primary particles of the powders calcined at 500°C were uniform and about 10 nm in size. These results are in agreement with those calculated from broadening of the XRD peaks by Scherrer's equation.

SEM micrographs of the calcined titania nanoparticles are shown in Fig. 5. The SEM samples were prepared by calcining the titania particles at 200–900°C for 2 hours in air. As shown in Fig. 5a, the powders calcined at 200°C were composed of spherical secondary particles that are about 20 nm in size and agglomerates of finer primary particles. It is hard to identify in Fig. 5a the primary particles since grain growth does not occur at a low temperature of 200°C. An increase in calcination temperature from 200 to 500°C resulted in the formation of the crystalline primary particles due to crystal growth as shown in Fig. 5b. The secondary particles were grown to 40–50 nm in size. As the calcination temperature was further increased to 700°C, the crystalline primary particles were observed clearly in the agglomerated secondary particles whose size was actually unchanged in comparison to that obtained at 500°C. It is interesting to note in Fig. 5d that the size of the secondary particles increased considerably to 200–400 nm at a temperature of 900°C. Furthermore, the secondary particles became highly densified and had a

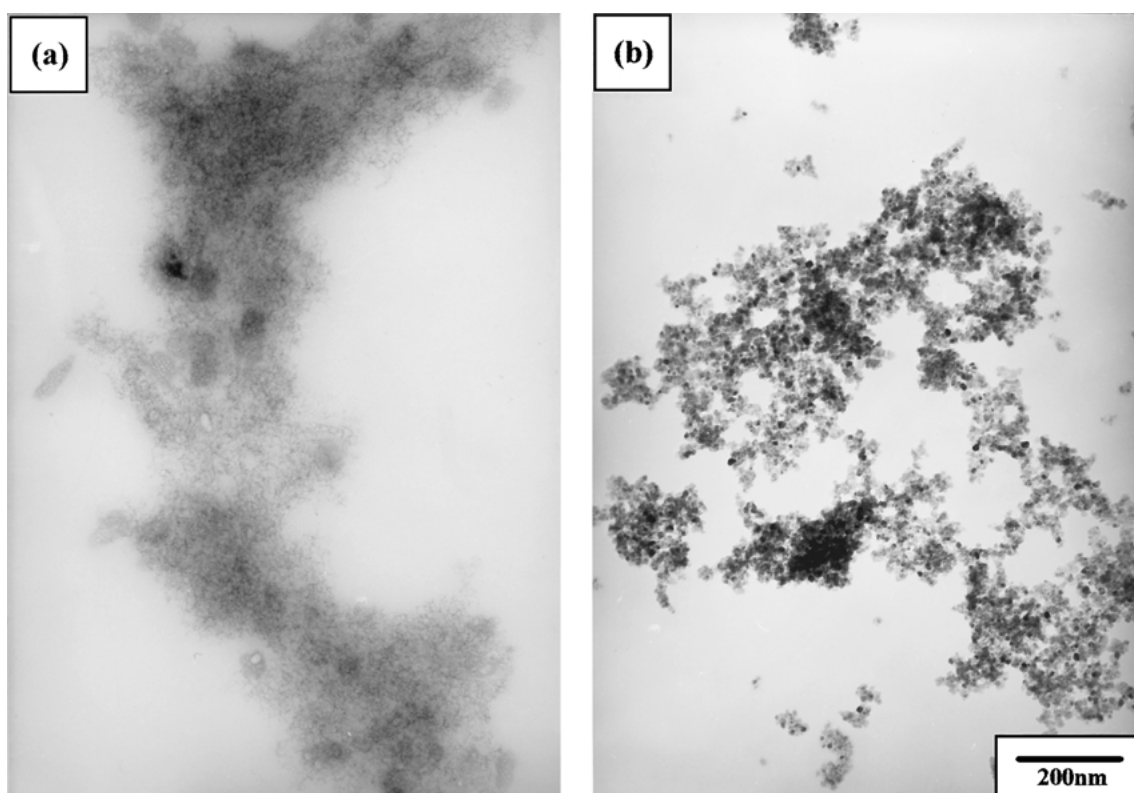


Figure 4 TEM micrographs of titania particles: (a) as-prepared; (b) at 500°C.

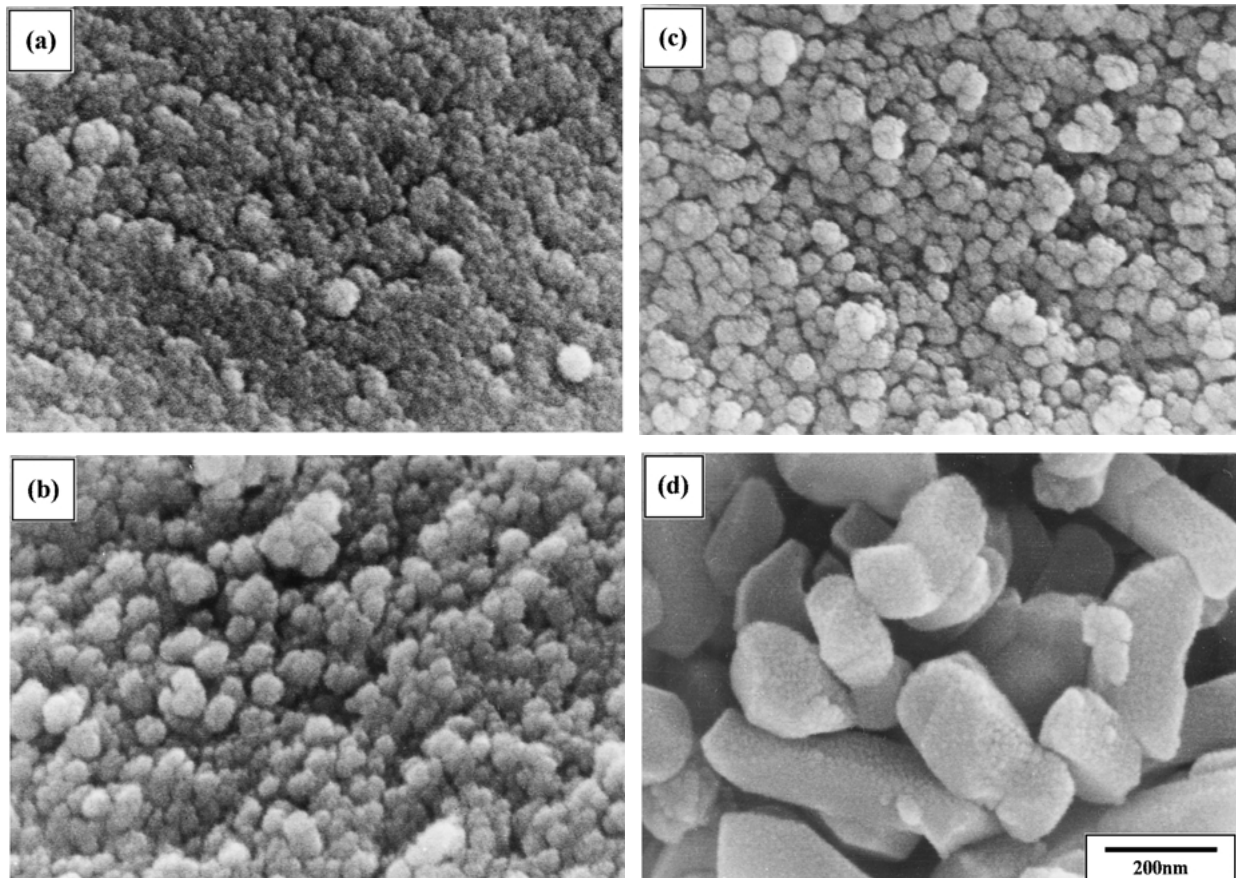


Figure 5 SEM micrographs of titania particles calcined at (a) 200°C; (b) 500°C; (c) 700°C; (d) 900°C.

nonspherical shape. However, the size of the primary particles comprising the secondary particles was increased only about twice relative to 700°C, which was confirmed by the XRD results.

Hague *et al.* [19] observed that as nanocrystalline titania particles were calcined at about 600°C, anatase crystals within agglomerates became sintered, thus the crystals grew through coalescence thereby transforming the original agglomerate into a single anatase grain. They also found that once the anatase-rutile transformation was complete, the rutile grain size was much larger than the original agglomerate and no longer nanocrystalline. Porter *et al.* [17] reported that the grain size of Degussa P-25 powders was increased by a factor of 10 as the calcination temperature increased from 600 to 900°C. In this work, however, rapid grain growth leading to a larger single grain greater than 100 nm was not observed at a temperature up to 900°C. SEM micrographs in Fig. 5 showed that as the calcination temperature was increased from 200 to 900°C, the size of secondary particles, agglomerates of the ultrafine particles, increased considerably by a factor of 10 to 20, whereas the size of the primary particles increased about 3.5 times. The SEM and XRD results obtained here indicate that the crystals of titania particles prepared in W/O microemulsions grew largely by intra-agglomerate densification below 850°C, whereas the particles grew by interagglomerate densification at 900°C. It is notable in Fig. 5d that the primary particle identity still remained in the agglomerates at 900°C.

The specific surface area and average pore radius of the titania particles are plotted in Fig. 6 as a func-

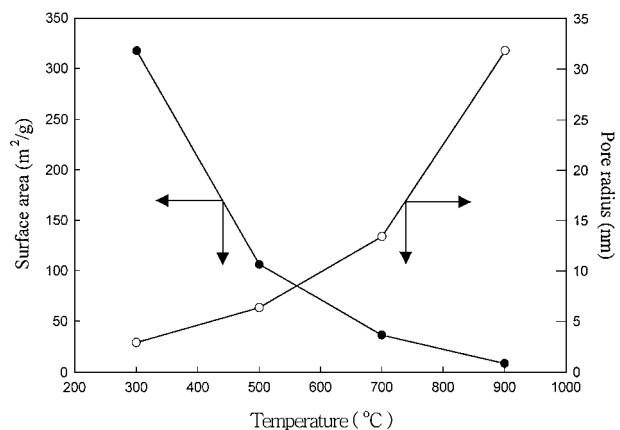


Figure 6 Effect of calcination on the specific surface area and average pore radius of titania particles.

tion of calcination temperature. It can be seen in Fig. 6 that the specific surface area decreased rapidly from 318.5 to 8.4 m<sup>2</sup>/g as the temperature was increased from 300 to 900°C. Chhabra *et al.* [10] observed a similar trend in their experiments. The pore volume was also found to decrease appreciably from  $4.62 \times 10^{-7}$  to  $1.33 \times 10^{-7}$  m<sup>3</sup>/g with increasing temperature from 300 to 900°C. The appreciable drop in pore volume with calcination temperature is attributable to elimination of the interagglomerate pores leading to an increase in the size of the secondary particles. As seen in Fig. 6, the average pore radius increased considerably from 2.9 to 31.8 nm by a factor of 10. Under calcination at higher temperatures, the surface area becomes largely external to the agglomerates since the small pores inside the

agglomerates have higher sintering rates [20]. An increase in calcination temperature facilitates shrinkage of the agglomerates, destruction of the intercrystallite pores, and interagglomerate densification. As a result, large dense secondary particles are formed at 900°C as noted above in the SEM micrographs.

#### 4. Conclusion

In this work, monodispersed titania nanoparticles were synthesized from reacting  $\text{TiOCl}_2$  with  $\text{NH}_4\text{OH}$  in the aqueous cores of water/Triton X-100/*n*-hexanol/cyclohexane microemulsions. The effect of calcination on the microstructure of the titania particles was examined using FTIR, XRD, SEM, TEM, and BET techniques. The XRD results showed that the particles precipitated were amorphous, transformed into the metastable anatase phase at 300°C and further into the stable rutile phase at 850°C. Comparison of our results and those of Chhabra *et al.* [10] reveals that higher reactant concentrations promote the transition of anatase to rutile lowering the phase transition temperature. The size of anatase crystallites increased about 3 times as the temperature was increased from 300 to 850°C. The size of rutile crystallites obtained at 900°C was found to be 35.6 nm, which is slightly greater than that obtained at 850°C. Thus, rapid intra-agglomerate grain growth leading to a huge single grain did not occur up to 900°C. The secondary particles, agglomerates of the primary particles, increased markedly by a factor of 10 to 20 with increasing temperature from 200 to 900°C, owing to a considerable interagglomerate densification. As the calcination temperature was increased, the specific surface area of titania particles decreased rapidly, whereas the average pore radius increased significantly due to shrinking of the agglomerates, destruction of the minute intercrystallite pores, and interagglomerate densification.

#### Acknowledgments

The authors wish to acknowledge the financial support of the University of Ulsan made in the program year

of 1999. The authors also would like to thank Korea Basic Science Institute (Taegu Branch) for XRD, SEM, and TEM measurements, and SK Corporation for BET measurements.

#### References

1. E. MATIJEVIC, M. BUDNIK and L. MEITES, *J. Colloid Interface Sci.* **6** (1977) 302.
2. M. FORMENTI, F. JUILLET, P. MERIAUDEAU, S. J. TEICHNER and P. VERGNON, *ibid.* **39** (1972) 79.
3. Y. SUYAMA and A. KATO, *J. Amer. Ceram. Soc.* **7** (1976) 63.
4. J. H. JEAN and T. A. RING, *Colloids Surf.* **29** (1988) 273.
5. E. A. BARRINGER and H. K. BOWEN, *Langmuir* **1** (1985) 414.
6. J. L. LOOK and C. F. ZUKOSKI, *J. Amer. Ceram. Soc.* **75** (1992) 1587.
7. H. K. PARK, D. K. KIM and C. H. KIM, *ibid.* **80** (1997) 743.
8. C. BECK, W. HÄRTL and R. HEMPELMANN, *J. Mater. Res.* **13** (1998) 3174.
9. F. J. ARRIAGADA and K. OSSEO-ASARE, *J. Colloid Interface Sci.* **211** (1999) 210.
10. V. CHHABRA, V. PILLAI, B. K. MISHRA, A. MORRONE and D. O. SHAH, *Langmuir* **11** (1995) 3307.
11. S.-J. KIM, S.-D. PARK, Y. H. JEONG and S. PARK, *J. Amer. Ceram. Soc.* **82** (1999) 927.
12. P. FIRMAN, D. HAASE, J. JEN, M. KAHLWEIT and R. STREY, *Langmuir* **1** (1985) 718.
13. R. D. SHANNON and J. A. PASK, *J. Amer. Ceram. Soc.* **48** (1965) 1391.
14. M. LAL, V. CHHABRA, P. AYYUB and A. MAITRA, *J. Mater. Res.* **13** (1998) 1249.
15. S. A. GREENBERG, *J. Phys. Chem.* **61** (1957) 960.
16. B. D. CULLITY, "Elements of X-Ray Diffraction," 2nd ed. (Addison-Wesley, Reading, MA, 1978) p. 94.
17. J. F. PORTER, Y.-G. LI and C. K. CHAN, *J. Mater. Sci.* **34** (1999) 1523.
18. L. H. EDELSON and A. M. GLAESER, *J. Amer. Ceram. Soc.* **71** (1988) 225.
19. D. C. HAGUE and M. J. MAYO, *Nanostructured Materials* **3** (1993) 61.
20. W. WAGNER, R. S. AVERBACK, H. HAHN, W. PETRY and A. WIEDENMANN, *J. Mater. Res.* **6** (1991) 2193.

Received 27 June

and accepted 2 November 2001